

SYNTHESIS & CHARACTERIZATION OF STYRENE-DIVINYLBASED MOLECULARLY IMPRINTED POLYMER FOR THE REMEDIATION OF PHTHALATE CONTAMINATED WASTEWATER

K. N. AWOKOYA*, V. O. ONINLA, A. O. OGUNFOWOKAN, C. O. ADEKOYA & A. I. AKINJOKUN

(K. N. A., V. O. O., A. O. O. & C. O. A. :Department of Chemistry, Obafemi Awolowo University, Ile-Ife, Nigeria; A. I. A. : Department of Chemical Sciences, Joseph Ayo Babalola University, Ikeji-Arakeji, Nigeria)

*Corresponding Author's email: knawokoya@oauife.edu.ng; knawokoya@gmail.com

ABSTRACT

Here, a series of molecularly imprinted polymers (MIPs) were synthesized using dibutyl & diphenyl phthalates as templates with bulk polymerization method. The MIPs were employed for phthalates removal from wastewaters of environmental importance & characterized by XRD, SEM & FTIR. The designed experiments were carried out to explore the adsorption thermodynamics, kinetics & isotherms. The adsorbents were featured with excellent *DBP* and *DPhP* adsorption efficiencies that exceeded 90%. The pseudo-second order kinetic model is more consistent with the experimental data, whilst the adsorption data was well explained by Langmuir isotherm model, suggesting homogeneous surface of the adsorbent. In addition, the calculated thermodynamic parameters revealed that the adsorption process was mainly spontaneous & endothermic in nature, with favourable adsorption efficiencies at elevated temperatures. The sorbent also showed no adsorption efficiency loss even after seven (7) runs of regeneration cycle, indicating that it is of great stability & could be considered as a candidate with excellent potential for complex wastewater treatment. Finally, this study demonstrated that phthalates in wastewaters could be effectively adsorbed by imprinted material.

Keywords: Adsorption, phthalates, characterization, molecular imprinted polymers, phthalate sequestration

Introduction

The contamination of water resources with phthalates poses a potential health risk to humans because of their xeno-estrogen-like activities, mutagenic & carcinogenic effects (Nielson & Larsen, 1996). Phthalates, are regarded as a group of endocrine disrupting compounds with a wide spectrum of industrial applications. They are commonly used as plasticizers in many personal-care products such as lotions, cosmetics &

perfumes. They are also utilized as viscosity controllers, binders, gelling agents, film formers & in making lacquers etc. (Heo, *et al.*, 2020). Among the different phthalates, dibutyl phthalate (DBP) with molecular formula, $C_{16}H_{22}O_4$ & diphenyl phthalate (DPhP) with molecular formula, $C_{20}H_{14}O_4$ are a large class of phthalates used as ectoparasiticides, & have attracted significant attention in environmental protection & food safety. In addition, the

U.S. Environmental Protection Agency (EPA) has also identified DBP as one of the priority pollutants (Heo, *et al.*, 2020). Therefore, it is of great importance to remove both *DBP* and *DPhP* from aqueous medium employing effective techniques. From the literature, the reported removal methods include adsorption, chemical precipitation, coagulation, photodegradation, reverse osmosis, flocculation, ion exchange, electrochemical treatment (Schoonenberg Kegel *et al.*, 2010; Guo *et al.*, 2013; Qi *et al.*, 2015; Asfaram *et al.*, 2016; Awokoya *et al.*, 2017; Tang *et al.*, 2021; Brito *et al.*, 2021). Most of the techniques are efficient but costly & time-consuming. Among these techniques, adsorption is considered cost effective, high performance process, flexibility in operation & promising technique due to its compatibility with the environment & wide range of application (Zhao *et al.*, 2010; Shen *et al.*, 2011). Recently, the development of adsorbents for water remediation has attracted increasing attention from researchers. Several adsorbents such as plant stems, pineapple leaf, clay, coconut husk, sugarcane pulp ash, rice husk ash activated carbon, zeolite, banana peels, wood apple shells, orange peels, peanut husk, peat, corn stalk, grapefruit peels & spent mushroom waste etc. have been extensively used for the removal various classes of pollutants from aqueous medium (Allen *et al.*, 2004; Arami *et al.*, 2005; Han *et al.*, 2008; Jain & Sikarwar 2008; Saeed *et al.*, 2010; Sadaf & Bhatti 2014; Bijari *et al.*, 2018; Munagapati *et al.*, 2018; Mousavi *et al.*, 2020), but many of these adsorbents have limited applicability because their non selective, low adsorption capacity, and attrition. Therefore, to address these limitations, adsorbent with unique characteristics of selectivity, high

mechanical strength, high adsorption capacity, long shelf life is needed. In line with this, molecularly imprinted polymers (MIPs) were employed. MIPs are synthetic polymeric and superior versatile adsorbents that have cavities specific to the target molecule (Vasapollo *et al.*, 2011). These MIPs are prepared by mixing a functional monomer with a template molecule (analyte) in the presence of a cross-linking agent to stabilize the three-dimensional structure of the MIP. After the polymerization, a thorough wash is used to remove the template, creating predicated imprinting's that are complementary to the template's shape and size (Awokoya *et al.*, 2022). In this present study, a novel styrene-divinyl based imprinted dibutyl and diphenyl phthalates MIPs were synthesized for the remediation of *DBP* and *DPhP* from wastewater. Styrene, has been used in this study as a suitable functional monomer to establish $\pi - \pi$ interaction with *DBP* and *DPhP* template molecules. The $\pi - \pi$ stacking interactions help the formation of imprinting sites on the polymer matrix, thus playing a more dynamic role in the removal of *DBP* and *DPhP* analytes. The aim of the present work was to assess and evaluate the performance of MIPs for the removal of *DBP* and *DPhP*, plasticizers used worldwide, through adsorption technique in a batch model. The prepared MIPs were also characterized using various analytical methods including Fourier transform infrared spectroscopy (FTIR), scanning electron microscopy (SEM), and X-ray powder diffraction (XRD) technique. In addition, the operating factors on the uptake of the phthalates, as well as kinetic, equilibrium isotherm and thermodynamic parameters were determined. The reusability and validation of the imprinted adsorbent were also studied to economize and validate

the method. To our knowledge, there are lacks of research done on styrene-divinyl based imprinted adsorbent for phthalates removal to date.

Experimentation

Materials

Dichloromethane, Divinyl benzene (DVB), styrene, benzoyl peroxide (BPO), Dibutyl and diphenyl phthalates were purchased from Sigma-Aldrich, Germany. Acetic acid and methanol were purchased from BDH, Poole, England. All chemicals and reagents were utilized as purchased without any further purification. Industrial wastewater was sourced from an industrial effluent's channel in Ibadan, Nigeria; river water was obtained from the Opa river, Ile-Ife, Nigeria; dumping site water sample was taken from a slowly flowing stream around a public dumping site in Ibadan, Nigeria. Distilled water was supplied by the Department of Chemistry, Obafemi Awolowo University, Ile-Ife, Nigeria.

Instrumentation

The XRD measurements were recorded using X-ray diffractometer (Bruker D8 Advance, Germany) in the range of $2\theta = 5 - 80 \text{ \AA}$ with a Cu K_{α} radiation source and scan speed of $5^{\circ}/\text{min}$ at room temperature. The polymers surface morphology was examined by a concise scanning electron microscopy (FEGSEM, model: 6100 Zeiss ultra plus, Germany). Functional groups present on the surface of the polymers were investigated using $FT - IR$ (Nicolet 330 spectrometer, Thermo Fisher Scientific, USA) at room temperature at a wavenumber range of $500 - 4000 \text{ cm}^{-1}$.

Synthesis of polymers (MIP_{DBP}/MIP_{DPhP})

The synthesis of the two different MIPs was carried out via Bulk polymerization method as reported by Awokoya *et al.*, 2021 with slight modification. The two prepared MIPs contained different template molecules. The template molecules, initiator, functional monomer, and crosslinker used in this synthesis were *DBP and DPhP* (one per MIP), BPO, styrene, and DVB, respectively. Exactly 520 mmol of styrene, 417 mmol of DVB, 1.078 μmol of *DBP*, 1.066 μmol *DPhP* and benzoyl peroxide (15 mg) were measured into a 100 mL reaction flask with magnetic stirring at 350 rpm until complete dissolution of all the solids. Afterwards, the polymerization reaction was carried out on a thermostatic heating module set at $70 \text{ }^{\circ}\text{C}$ for 18 h. After polymerization, the obtained polymers (MIP_{DBP}/MIP_{DPhP}) were crushed in a mortar and separately stored in an air-tight containers for further use.

As a reference, non-imprinted polymers (NIPs) were also synthesized via a similar method but without the presence of *DBP and DPhP* template molecules.

Template removal

The extraction of the templates from the MIP_{DBP} and MIP_{DPhP} was carried out as described by Awokoya *et al.*, 2021, but with slight modification. Both polymers (MIP_{DBP} and MIP_{DPhP}) were exhaustively washed with a mixture of methanol (MeOH) and acetic acid (9:1 v/v). Centrifugation of the mixture was performed and the absorbance of the supernatant obtained was taken (at 264 nm for *DBP* and 274 nm for *hP*) using a Shimadzu UV-Vis-1800 model Spectrophotometer (Canby, Oregon, USA). The obtained polymers were stored at room temperature for further characterisation.

Rebinding Studies for DBP and DPhP

Rebinding experiment was performed to determine the extent of *DBP and DPhP* removal and the adsorption capacity. The experiment was conducted by batch experimental technique on a speed-controllable thermostatic shaker (GFL, Burgwedel, Germany). Influence of parameters like contact (agitation) time, initial concentration of phthalates and temperature on the adsorption performance of the MIPs were investigated. In order to determine the optimum contact time for the adsorption process, 20 mL of 50 mg L⁻¹ solution of appropriate phthalate was used. These experiments were carried out by varying: contact time from 5 – 180 min using 50 mg adsorbent dosage. In the same way, different 50 mg quantity of the corresponding MIP was added to the phthalate solution with initial concentrations ranging from 5 to 100 µg L⁻¹ in the 120 mL glass vials and then arranged inside the shaker and allow to agitate for 90 min optimum time. The supernatant was separated by centrifugation at 6000 rpm for 10 min, and the MIP phthalate removal efficiency was determined by measuring the residual DBP or DPhP concentrations in the supernatant using a Shimadzu UV-Vis-1800 model Spectrophotometer (Canby, Oregon, USA) at the wavelength of 264 and 274 nm for *DBP and DPhP*, respectively.

The study on the effect of temperature was carried out at the established optimum time using 50 µg L⁻¹ of phthalate. This experiment was carried out by varying: temperature from 10 to 30 °C. Control experiments were similarly conducted using the NIP as adsorbent. The reusability of the MIPs was investigated by seven (7) cycle of repeated adsorption-desorption experiments.

Desorption experiment was performed by using a mixture of MeOH and acetic acid (9:1). The quantity of dye adsorbed per unit adsorbent (q_e (mg g⁻¹)) and percent phthalate removal (%) were calculated according to equations 1 and 2:

$$q_e = \frac{(C_o - C_e)V}{m} \quad 1$$

$$\% \text{ removal} = \frac{C_o - C_e}{C_o} \times 100 \quad 2$$

where C_o and C_e (in mg L⁻¹) stand for initial and equilibrium *DBP/DPhP* concentrations, respectively; m (g) stands for MIP / NIP mass; and V (L) represents volume of the solution. All studies were carried out in triplicate.

Equilibrium, Kinetic, and thermodynamic modeling

For better insight into the adsorption rate, the mass transfer parameters, the time required for the process to reach equilibrium, and the feasibility of the phthalates removal process, data generated from the adsorption experiment were fitted into four different kinetic models, namely: pseudo-first order, pseudo-second order, Weber Morris (Weber & Morris, 1963), and Elovich (Lagergren 1898; Ho & McKay, 1999). The relation between equilibrium mechanism, surface properties, adsorption behaviour, and affinity of adsorbents was investigated using adsorption isothermal models, namely, Langmuir, Freundlich (Freundlich, 1906; Langmuir, 1918; Singh & Mishra, 2010), Dubinin-Radushkevich (D-R) (Dubinin *et al.*, 1947) and Temkin (Temkin & Pyzhev, 1940).

The linearized forms of the models are as shown in Table 1. To investigate the adsorption thermodynamics, data were fitted

into the van't Hoff's equation (eq. 3). A linear plot of the equation was obtained, from whose slope and intercept the standard enthalpy (ΔH°) and standard entropy (ΔS°) of adsorption were respectively calculated. Estimation of the Gibb's free energy (ΔG°) was performed according to the thermodynamic relationship presented in eq. 4.

$$\ln K_c = \frac{\Delta S^\circ}{R} - \frac{\Delta H^\circ}{RT} \quad 3$$

$$\Delta G^\circ = \Delta H^\circ - T\Delta S^\circ \quad 4$$

The equilibrium constant, K_c , is defined as $\frac{C_a}{C_e}$ (C_a represents the concentration of the *DBP/DPhP* on the polymer); the gas constant is represented by ($8.314 \text{ J mol}^{-1} \text{ K}^{-1}$); whereas, T represents temperature in Kelvin (K); ε : Polanyi potential; β : (mol^2/kJ^2); B : Temkin constant; K_T : Temkin adsorption potential.

TABLE 1

Kinetic and isothermal model equations and the definition of their parameters.

Model Name	Model Type	Model Equation
PFO	Kinetic	$\ln (q_e - q_t) = \ln q_e - k_1 t$
PSO	Kinetic	$\frac{t}{q_t} = \frac{t}{q_e} - \frac{1}{k_2 q_e^2}$
W-M	Kinetic	$q_t = k_\alpha t^{1/2} + C$
Elovich	Kinetic	$q_t = \frac{1}{\beta} \ln[\alpha\beta] + \frac{1}{\beta} \ln t$
Langmuir	Isothermal	$\frac{1}{q_e} = \frac{1}{q_{\max} K_{LC_e}} + \frac{1}{q_{\max}}$
Freundlich	Isothermal	$\ln q_e = \ln k_f + \frac{1}{n} \ln C_e$
D-R	Isothermal	$\ln q_e = \ln q_m - \beta \varepsilon^2$ Where $\varepsilon = RT \ln \left(1 + \frac{1}{C_e}\right)$
Temkin	Isothermal	$q_e = b_T \ln K_T + b_T \ln C_e$

Where q_e and q_t (in $\mu\text{g g}^{-1}$) denote equilibrium *DBP/DPhP* adsorbed; t (min) represents adsorption time; k_1 (min^{-1}) and k_2 ($\text{g } \mu\text{g}^{-1} \text{ min}^{-1}$) respectively denote the pseudo-first order and pseudo-second order rate constants; α ($\mu\text{g min}^{-1}$) and β ($\text{g } \mu\text{g}^{-1}$) are constants respectively showing the initial adsorption rate at contact time $t = 0$ min, and the

extent of surface coverage; $k\alpha$ ($\text{mmol/g min}^{1/2}$) is the W-M rate constant; C : intercept; C_e (mg L^{-1}) denote the *DBP/DPhP* concentration at equilibrium; q_{\max} ($\mu\text{g g}^{-1}$) represents maximum adsorption capacity; K_a ($\text{L } \mu\text{g}^{-1}$) and k_f ($\mu\text{g g}^{-1}$) signify Langmuir and Freundlich constants, respectively; while n denote Freundlich intensity constant.

Application of MIP_{DBP} and MIP_{DPhP} to real samples

The synthesised MIPs were applied to industrial water (taken from an industrial effluent's channel), river water and ground water from a dumping site to investigate the efficiency of the material in real polluted water application. An appropriate volume (50 mL) of the polluted water was separately measured into a 250 mL separating funnel containing 50 mL dichloromethane. The separating funnel was vigorously shaken in order to allow the leaching of the organic component in the wastewater. The aqueous layer was separated from the organic layer by standing the separating funnel. The concentrations of both phthalates in the organic layer were determined by UV-visible spectroscopy. Adsorption of the phthalates was performed as earlier described. Amount of phthalate adsorbed was also determined by UV-visible spectroscopy.

Results and discussions

Adsorbents characterization

FT – IR spectra

The FT – IR spectra of MIP_{DPhP}, MIP_{DBP} and NIP are illustrated in Fig. 1a.

The analyses were used to determine the functional group present in the polymer materials. All the spectra revealed peaks at 1610, 1722, and 2918 cm^{-1} which are ascribed to $C = C$, $C = O$ and CH_2 , respectively. The $C = O$ peak observed at 1722 cm^{-1} was found to be present in the spectra of both the NIPs and MIPs. This strongly implies that the peak is unlikely to represent the carbonyl group from the phthalates, but rather the carbonyl group of the benzoyl peroxide initiator moiety. Also, the band around 1610 cm^{-1} can be assigned to $C = C$ aromatic peak which demonstrates that the styrene functional monomer and divinyl benzene crosslinker were included in the pre-polymerization mixture. In addition, the similarity in the back bone structure of all the spectra proves that the mixture contained the same chemical components and complete extraction of template molecule from the MIP. The band around 2918 cm^{-1} represent $C - H$ vibration stretching in the methylene group. Some other minor peaks around 842 and 905 cm^{-1} were also observed in the polymers investigated, these bands can be attributed to $C - H$ twisting, and $C - H$ wagging, respectively (Bhawani *et al.*, 2020).

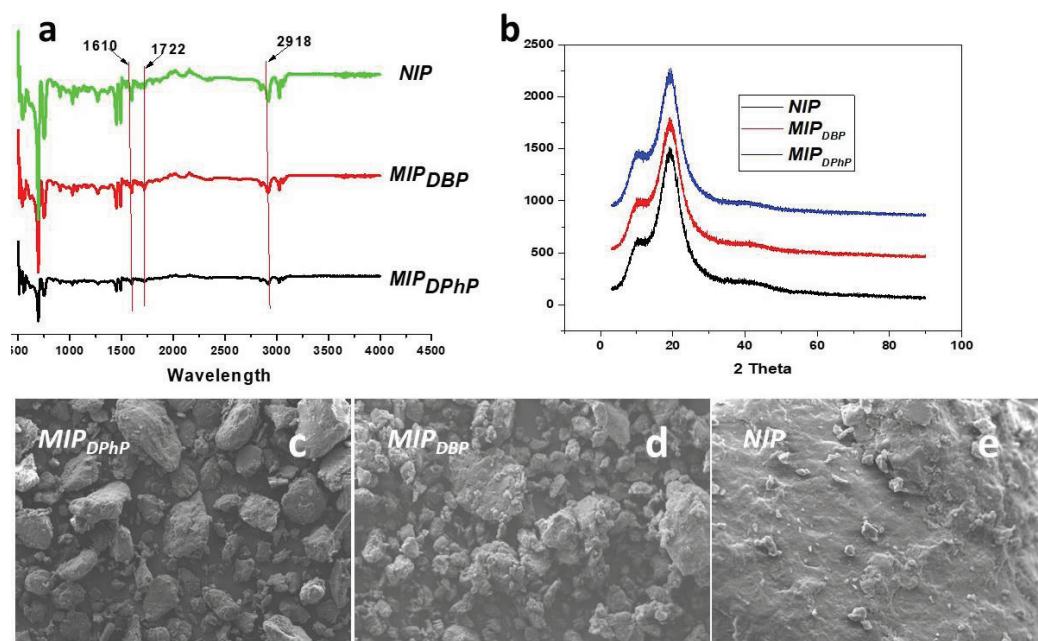


Fig.1: FT-IR spectra (a), X-ray diffraction curves of the polymers (b) and SEM images (c-e)
XRD pattern

To have information on the crystallinity of the synthesized polymers, the XRD data can be helpful. X-ray diffraction patterns for MIP_{DPhP} , MIP_{DBP} and NIP are presented in Fig. 1b. The diffraction patterns depicted well-defined and similar peaks (2θ) at 10.09° and 20.03° , which describes the crystalline nature of the three adsorbents. The diffractograms for all the polymers suggest that the three adsorbents contained substantial amount of glassy amorphous phase, thus we can conclude that amorphous nature of the adsorbents is good for adsorption (Yakun, *et al.*, 2011).

SEM

The surface morphologies of synthesized MIP_{DPhP} , MIP_{DBP} and NIP were characterized by SEM. As presented in Fig. 1c and d, the surfaces of MIP_{DPhP} and MIP_{DBP} were rough with a grain-like

porous surfaces. This is evidence that the template molecules (DBP and $DPhP$) have been re-imprinted on the cavities initially created by the leaching of the template from the surface of the MIPs. On the other hand, the NIP (Fig. 1e) showed a smooth and homogeneous surface with well-dispersed particles on the surface. This phenomenon occurred because no template was imprinted on the NIP material. This observation is consistent with the previous studies in the literatures (Yongfeng, *et al.*, 2012; Khatibi, *et al.*, 2021).

Adsorption of DBP and $DPhP$

Effect of contact time on DBP and $DPhP$ uptake and kinetic study

The experiments on the influence of contact time on DBP and $DPhP$ uptake was

performed from 5 to 180 min. The set condition for the study involved $50 \mu\text{g L}^{-1}$ phthalates concentration, 0.05 g adsorbent dose, room temperature, and 200 rpm agitation speed. As presented in Fig. 2A, the percentage adsorption increased gradually with increase in time up till 90 min for all the adsorbents (MIPs and NIP). The phthalates adsorption was rapid in the first 40 min. The removal of the phthalates in the aqueous system with MIP_{DBP} , MIP_{DPhP} , NIP_{DBP} and NIP_{DPhP} was 96.21, 86.00, 51.98, and 44.67% respectively within 60 min. As can be seen, with the increase of time from 60 to 90 min, the % adsorption increased at first and then reached saturation. There was no significant change in % adsorption after 90 min. The highest percentage (99.3%) was achieved for MIP_{DBP} , 89.4% for MIP_{DPhP} , 54.08% for NIP_{DBP} , and 47.69% for NIP_{DPhP} when the time was between 90 to 180 min. Based on these results, agitation time of 90 min was adopted for all subsequent experiments. To evaluate the kinetics of the adsorption of *DBP and DPhP*, *pseudo – first – order*, *pseudo – second – order*, *Weber – Morris*, and *Elovich* models were used to

fit the experimental data. The results are as presented in Table 2. The *pseudo – first – order*, *Weber – Morris* and *Elovich* models were found to be inefficient to describe the experimental data. The adsorption process was most appropriately described by the *pseudo – second – order* model. This was informed by the regression coefficients, $R^2 = 0.7884 - 0.9499$ obtained from the three models whose values were relatively lower, when compared with the values obtained from the *pseudo – second – order (PSO)* model ($R^2 = 0.9603 - 0.9995$). This indicates that the adsorption rate was dependent on both the adsorbate and adsorbent. It is also noticeable that the $q_{e(cal)}$ for *PSO* was very close to that obtained experimentally. This further shows that the adsorption follows the *PSO* mechanism. In addition, the elovich kinetic parameters obtained in this study ascertain that the adsorption rate of *DBP and DPhP* molecules onto MIPs/NIPs was greater than their desorption rate ($\alpha > \beta$). A similar trend was reported by Abd El-Monaem *et al.*, 2023 on congo red adsorption onto chitosan Schiff base materials.

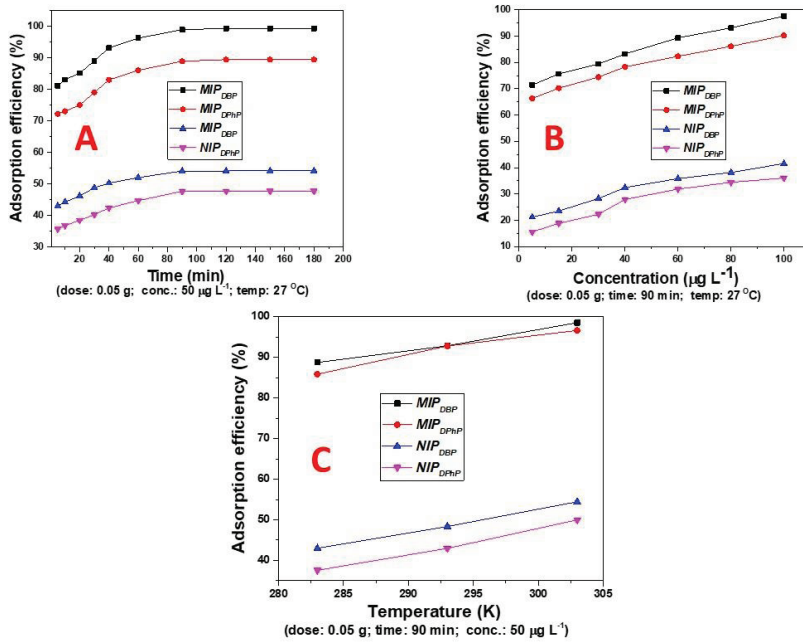


Fig. 2: The effect of time (A), Initial concentration (B) and temperature (C)

TABLE 2

Linearized kinetic model equations and the values of parameters calculated from their plots
(PFO pseudo – first – order, PSO pseudo – second – order, Weber – Morris & Elovich)

Kinetic Model	Linearized equation	Parameter	MIP_{DBP}	MIP_{DPhP}	NIP_{DBP}	NIP_{DPhP}
PFO	$\ln(q_e - q_t) = \ln q_e - k_1 t$	R^2	0.9361	0.8129	0.9355	0.9375
		$k_1 (L \text{ min}^{-1})$	0.0537	0.0353	0.0448	0.0386
		$q_{e(\text{exp})} (\mu\text{g g}^{-1})$	15.0196	13.1673	5.8300	2.2400
		$q_{e(\text{calc})} (\mu\text{g g}^{-1})$	14.0419	13.2285	5.8402	2.2421
		R^2	0.9995	0.9990	0.9963	0.9603
PSO	$\frac{t}{q_t} = \frac{t}{q_e} - \frac{1}{k_2 q_e^2}$	$k_2 (g \mu\text{g}^{-1} \text{ min}^{-1})$	0.0139	0.0301	0.1921	0.0034
		$q_{e(\text{exp})} (\mu\text{g g}^{-1})$	14.0196	13.1673	5.8300	2.2400
		$q_{e(\text{calc})} (\mu\text{g g}^{-1})$	14.0286	13.4505	6.0092	3.3383
		R^2	0.9499	0.8845	0.9499	0.7884
		$k_\alpha (\mu\text{g g}^{-1} \text{ min}^{-1/2})$	0.2287	0.2067	0.2287	0.0868
W-M	$q_t = k_\alpha t^{1/2} + C$	R^2	10.611	12.028	2.846	12.557
		C	0.9380	0.9491	0.9380	0.8844
		α	3.21E+5	8.5090	2.7500	1.2E+2
		β	1.3569	0.8732	1.3569	1.6213
		R^2	0.9380	0.9491	0.9380	0.8844
Elovich	$q_t = \frac{1}{\beta} \ln[\alpha\beta] + \frac{1}{\beta} \ln t$	R^2	0.9380	0.9491	0.9380	0.8844
		α	3.21E+5	8.5090	2.7500	1.2E+2
		β	1.3569	0.8732	1.3569	1.6213
		R^2	0.9380	0.9491	0.9380	0.8844
		α	3.21E+5	8.5090	2.7500	1.2E+2

Effect of initial concentration and isotherm study

The effect of initial adsorbate concentration on *DBP* and *DPhP* removal is illustrated in Fig. 2B. The % sorption of both analytes, by imprinted materials (MIP_{DBP} & MIP_{DPhP}) and non-imprinted materials (NIP_{DBP} & NIP_{DPhP}), increased with rise in the initial concentration. The results apparently show that the imprinted materials have higher adsorption capacities when compared with their non-imprinted counterparts. The *DBP* adsorption capacity of the MIP_{DBP} (obtained as 97.56% at $100 \mu\text{g L}^{-1}$) was found to be about 2.4 times higher than that of the NIP_{DBP} (obtained as 41.57%); whilst the *DPhP* adsorption capacity of the MIP_{DPhP} (obtained as 90.22%) was about 2.5 times higher than that of the NIP_{DPhP} (obtained as 36.09%) at the same concentration. This result indicates that the cavities created by the imprinting technology act to enhance high adsorption performance. To further probe the interaction between the adsorbate and adsorbent, four common isotherm models; namely Langmuir, Freundlich, Dubinin-Radushkevich and Temkin models were applied to determine the one that can best describe the adsorption of *DBP* and *DPhP*.

The obtained equilibrium parameters are presented in Table 3. Results of the isothermal modeling suggest that the *DBP* and *DPhP* adsorption onto the polymer materials best fitted the Langmuir model, when compared with the other three models. The regression coefficients (R^2) obtained from the Langmuir model was in the range of 0.9906 – 0.9961. This indicates a homogeneous distribution of adsorption sites on the surfaces of the polymer materials. In addition, the results from the Langmuir model revealed that the calculated maximum adsorption capacities (q_{max}) of MIP_{DBP} , MIP_{DPhP} , NIP_{DBP} , and NIP_{DPhP} were 12.28, 7.27, 5.89, and $4.45 \mu\text{g g}^{-1}$, respectively. As expected, the q_{max} values of MIP_{DBP} and MIP_{DPhP} were higher than that of NIP_{DBP} , and NIP_{DPhP} . It should be noted that the q_{max} obtained in this study are higher than some of the literature-reported materials such as activated carbon (Al-Degs *et al.*, 2008), and multiwalled carbon nanotubes (Den *et al.*, 2006). Also, the Langmuir constant K_L , often related to the sorption energy has values higher than zero (0.3564 – 0.6200) which implied relatively good degree of adsorbate-adsorbent interaction.

TABLE 3

Linearized isothermal model equations and the values of parameters calculated from their plots

Isothermal Model	Linearized equation	Parameter	MIP_{DBP}	MIP_{DPhP}	NIP_{DBP}	NIP_{DPhP}
Langmuir	$\frac{1}{q_e} = \frac{1}{q_{max}K_{LC_e}} + \frac{1}{q_{max}}$	R^2	0.9915	0.9961	0.9906	0.9943
		$k_L (L \mu g^{-1})$	0.4230	0.6200	0.3564	0.5746
Freundlich	$\ln q_e = \ln k_f + \frac{1}{n} \ln C_e$	$q_{max}(\mu g g^{-1})$	12.2850	7.2670	5.8990	4.4532
		R^2	0.9107	0.8963	0.9235	0.8944
		$k_f (L \mu g^{-1})$	3.3902	2.6575	1.3357	1.0258
D-R	$\ln q_e = \ln q_m - \beta \varepsilon^2$	$1/n$	0.3477	0.2675	0.1165	0.1144
		R^2	0.9649	0.9650	0.9621	0.9711
		$q_m(\mu mol g^{-1})$	14.595	8.5910	6.8899	4.7452
Temkin	$q_e = B \ln K_T + B \ln C_e$	$E (kJ mol^{-1})$	8.4500	9.1290	9.6794	9.9958
		R^2	0.9897	0.9724	0.9757	0.9822
		$k_T (L \mu g^{-1})$	0.0066	0.0136	0.0189	0.0233
		$b (kJ mol^{-1})$	332.56	712.63	965.01	1022.04

Effect of temperature and thermodynamic study

The experiment on the effect of temperature on the adsorption of *DBP/DPhP* by the polymer materials was evaluated at adsorbent mass of 0.05 g, time of 90 min, and initial concentration of $50 \mu g L^{-1}$. As illustrated in Fig. 2C, by increasing the temperature from 283 to 303 K, the adsorption efficiency rose. For instance, the adsorption efficiency increased from 88.8% to 98.6%, 85.9 to 96.6%, 42.9 to 54.4%, and 37.6 to 49.9% for MIP_{DBP} , MIP_{DPhP} , NIP_{DBP} , and NIP_{DPhP} , respectively, with increase in temperature from 283 to 303 K, indicating that the sorption process was endothermic in nature. To evaluate the feasibility and orientation of *DBP/DPhP* adsorption by the polymers, the thermodynamics parameters were determined as shown in Table 3. Expectedly, ΔH° values as calculated from equation 4 were all positive, ($MIP_{DBP} =$

+29.09, $MIP_{DPhP} = +31.59$, $NIP_{DBP} = +21.33$, and $NIP_{DPhP} = +19.48 kJ mol^{-1}$), thus corroborating the endothermic nature of the process. The calculated ΔG° values were negative at all the temperatures examined, implying that the sorption process of *DBP/DPhP* by the adsorbent was spontaneous and feasible. In addition, the evidence of energetically spontaneous reaction and viability of the phthalates adsorption on the polymers was provided by the increase in negative values of ΔG° (Table 4) as temperature increased from 283 to 303 K. The positive values of ΔS° showed that the process was characterized by high degree of increasing randomness at the adsorbent-adsorbate interface during the sorption process. This result is in agreement with the study of Li *et al.*, 2020 who reported that the removal of dibutyl phthalate is an endothermic process using three common substrates.

TABLE 4

Thermodynamic parameters obtained for the adsorption of DBP and DPhP onto MIP_{DBP} , MIP_{DPhP} , NIP_{DBP} and NIP_{DPhP}

Parameter	Temperature (K)	MIP_{DBP}	MIP_{DPhP}	NIP_{DBP}	NIP_{DPhP}
ΔH ($kJmol^{-1}$)		29.095	31.596	21.331	19.482
ΔS ($kJmol^{-1}K^{-1}$)		0.103	0.116	0.125	0.183
ΔG ($kJmol^{-1}$)	283	-0.17	-1.24	-0.24	-1.37
	293	-1.21	-2.40	-1.33	-2.11
	303	-2.24	-3.56	-2.46	-3.77

Recycle performance

In practical and commercial applications, reusability and regeneration of adsorbents are considered to be critical parameters for assessing the adsorption performance. The recycling performance was evaluated using seven (7) successive adsorption-regeneration cycles, as depicted in Figure 3. From the results, it can be seen that the adsorption efficiencies of the MIP_{DBP} and MIP_{DPhP} were kept above 97% and 90%, respectively even after seven repeated uses. This implies that the imprinted materials exhibited acceptable reusability and had strong adsorption capacity after regeneration. Thus, the adsorbents developed in this study can be considered as an efficient candidate for the DBP and $DPhP$ sequestration from wastewater.

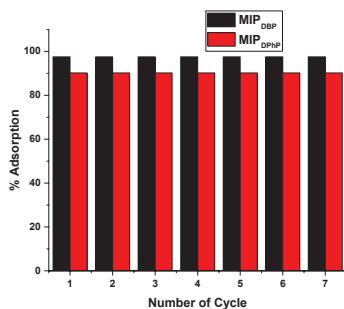


Fig. 3: Adsorption percentage of MIP for DBP and $DPhP$ in seven consecutive regeneration cycles

Efficiencies of MIP_{DBP} and MIP_{DPhP} in real samples

The determination of DBP and DPhP concentrations in real polluted water samples from three sources indicates the highest level of pollution in the industrial wastewater sample, with DBP and DPhP concentrations as high as 475.7 $\mu g/L$ and 427.6 $\mu g/L$, respectively. In water from dumping site, 135.9 $\mu g/L$ and 111.7 $\mu g/L$ were recorded for DBP and DPhP, respectively; while the concentrations of DBP and DPhP in water sample from river Opa were obtained as 59.9 $\mu g/L$ and 41.5 $\mu g/L$, respectively. The occurrence of the phthalates in both waters from dumping site and river Opa could partly be attributed to the leaching of the compounds from PET bottles and other plastic materials. The relatively low pollution level recorded in river water, however, could be as a result of the flowing nature of the water. As illustrated in Fig 4, upon adsorption, using 0.05 g dose of the appropriate adsorbents, the efficiency of MIP_{DBP} and MIP_{DPhP} in removing DBP and DPhP were respectively determined as: 57.9% and 69.9%, for industrial wastewater sample; 74.8% and 71.1% for sample of water taken from dumping site and; 85.1% and 79.3%, for river Opa water sample. The seemingly low efficiency of the

adsorbents in real polluted water could be attributed to (i) high pollutant concentrations in the real waters (ii) simultaneous adsorption of other compounds (pollutants other than DBP and DPhP) present in the real water samples and, (iii) high concentrations of DBP and DPhP in the real water compared to the chosen experimentally simulated concentration. Despite all the above listed factors, the relatively high efficiencies (57.9 – 85.1%) recorded in real water samples showed that the developed adsorbents were efficient and effective in the removal of DBP and DPhP – all that is needed is to increase the dosage of the adsorbents administered.

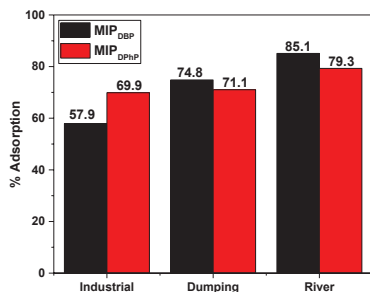


Fig. 4: Determination of DBP and DPhP industrial, dumping ground and river wastewaters

Conclusions

In summary, we report a styrene-divinyl based molecularly imprinted polymer for the removal of dibutyl and diphenyl phthalates with high adsorption efficiency and considerable reusability. The synthesized polymeric materials were characterized by FTIR, XRD and SEM. The adsorption percentages of DBP and DPhP were 2.4 and 2.5 times higher than that of the NIPs, respectively. It was found that the polymer showed fast kinetics, followed pseudo-second order kinetics model and fitted well to the Langmuir isotherm model

($R^2 = 0.9906 - 0.9961$), which indicates that the distribution of the adsorption sites was homogeneous. The thermodynamic parameters revealed that the adsorption process was endothermic, feasible, spontaneous, and have high degree of increasing randomness. The synthesized imprinted polymers (MIP_{DBP} and MIP_{DPhP}) were successfully applied to the real samples of industrial, dumping ground and river wastewaters, the results clearly demonstrated that MIPs could be effectively used as sorbents for real sample analysis. Overall, it was found that the MIPs have excellent adsorption efficiency, good versatility, and high stability for DBP and DPhP, thus, making the polymers promising adsorbents for adsorption of phthalates from wastewater.

Acknowledgments

The authors would like to express their sincere appreciation to the leadership of Polymer Science and Biophysical Laboratory, Department of Chemistry, Obafemi Awolowo University, Ile-Ife, Nigeria for access to their laboratory facilities.

Author contributions

Authors AOO and KNA were involved in the conception of the study. Authors VOO, KNA and COA were involved in data acquisition, processing, and interpretation. AOO, KNA, VOO and AIA were further involved in drafting the manuscript and making necessary revision. All authors reviewed and approved the manuscript for submission.

Funding

No funding was received for this study.

Availability of data and materials

Data and materials are available on request.

Declarations Conflicts of interest

The authors declare that there are no conflicts of interest.

Ethics approval

This research did not involve human subjects.

Consent to participate

This research did not involve human subjects.

Reference

- ABD EL-MONAEM, E.M., AYOUP, M.S., OMER, A.M., HAMMAD, E.N., & ELTAWEI, A.S. (2023). Sandwich-like construction of a new aminated chitosan Schiff base for efficient removal of Congo red. *Appl. Water Sci.* **13**, 67. <https://doi.org/10.1007/s13201-023-01866-w>
- AL-DEGS, Y.S., EL-BARGHOUSHI, M.I., EL-SHEIKH, A.H., & WALKER, G.M. (2008). Effect of solution pH, ionic strength, and temperature on adsorption behavior of reactive dyes on activated carbon. *Dyes and Pigments* **77**, 16-23.
- ALLEN, S.J., MCKAY, G., & PORTER, J.F. (2004). Adsorption isotherm models for basic dye adsorption by peat in single and binary component systems. *J. Colloid Interface Sci.* **280**, 322–333.
- ARAMI, M., LIMAEI, N.Y., MAHMOODI, N.M., & TABRIZI, N.S. (2005). Removal of dyes from colored textile wastewater by orange peel adsorbent: equilibrium & kinetic studies. *J. Colloid Interface Sci.* **288**, 371–376.
- ASFARAM, A., GHAEDI, M., GHEZELBASH, G.R., DIL, E.A., TYAGI, I., AGARWAL, S., & GUPTA, V.K. (2016). Biosorption of malachite green by novel biosorbent *Yarrowia lipolytica* *isf7*: application of response surface methodology. *J. Mol. Liq.* **214**, 249–258.
- AWOKOYA, K.N., OKOYA, A.A., & ELUJULO, O. (2021). Preparation, characterization & evaluation of a styrene-based molecularly imprinted polymer for capturing pyridine & pyrrole from crude oil. *Scientific African* **13**, 00947.
- AWOKOYA, K.N., ONINLA, V.O., ADEYINKA, G.C., AJADI, M.O., CHIDIMMA, O.T., FAKOLA, E.G., & AKINYELE, O.F. (2022). Experimental & computational studies of microwave-assisted watermelon rind –styrene based molecular imprinted polymer for the removal of malachite green from aqueous solution. *Scientific African* **16**, 01194.
- AWOKOYA, K.N., SANUSI, R.O., ONINLA, V.O., & AJIBADE, O.M. (2017). Activated periwinkle shells for the binding & recognition of heavy metal ions from aqueous media. *International Research Journal of Pure & Applied Chemistry*, **13**, 1-10.
- BHAWANI, S.A., BAKHTIAR, S., ROL&, R., SHAFQAT, S.R., & IBRAHIM, M.N.M. (2020). Synthesis of molecularly imprinted polymers of vanillic acid & extraction of vanillic acid from spiked blood serum. *Journal of Applied Pharmaceutical Science* **10**, 056-062. doi: 10.7324/JAPS.2020.104009.
- BIJARI, M., YOUNESI, H., & BAHRAMIFAR, N. (2018). Optimization of activated carbon production by using K₂CO₃ at different temperatures for the removal of reactive black 5 dye from aqueous solutions. *Iran J. Health Environ.* **10**, 483–500.
- BRITO, L.R., GANIYU, S.O., DOS SANTOS, E.V., OTURAN, M.A., & MARTÍNEZ-HUITLE, C.A. (2021). Removal of antibiotic rifampicin from aqueous media by advanced

- electrochemical oxidation: role of electrode materials, electrolytes & real water matrices. *Electrochim Acta* **396**, 139254.
- DEN, W., LIU, H.C., CHAN, S.F., KIN, K.T., & HUANG, C. (2006). Adsorption of phthalate esters with multiwalled carbon nanotubes & its applications. *Journal of Environmental Engineering & Management* **16**, 275-282. *Desalination & Water Treatment* **230**, 240–251. doi: 10.5004/dwt.2021.27396
- DUBININ, M.M., ZAVERINA, E., & RADUSHKEVICH, L. (1947). Sorption & structure of active carbons. I. Adsorption of organic vapors. *Zh. Fiz. Khim.* **21**, 151–162.
- FREUNDLICH, H.M.F. (1906). Uber die adsorption in lasungen. *Z. Phys. Chem.* **57**, 385–470.
- GUO, X., CAI, Y., WEI, Z., HOU, H., YANG, X., & WANG, Z. (2013). Treatment of diazo dye CI reactive black 5 in aqueous solution by combined process of interior microelectrolysis & ozonation. *Water Sci. Technol.* **67**, 1880–1885.
- HAN, R., DING, D., XU, Y., ZOU, W., WANG, Y., LI, Y., & ZOU, L. (2008). Use of rice husk for the adsorption of congo red from aqueous solution in column mode. *Bioresour Technol.* **99**, 2938–2946.
- HEO, H., CHOI, M.J., PARK, J., NAM, T., & CHO, J. (2020). Anthropogenic Occurrence of Phthalate Esters in Beach Seawater in the Southeast Coast Region, South Korea. *Water* **12**, 122. doi:10.3390/w1201012.
- HO, Y.S., & MCKAY, G. (1999). Pseudo-second order model for sorption processes. *Process Biochem.* **34**, 451–465. [http://dx.doi.org/10.1016/S0032-9592\(98\)00112-5](http://dx.doi.org/10.1016/S0032-9592(98)00112-5).
- JAIN, R., & SIKARWAR, S. (2008). Removal of hazardous dye congo red from waste material. *J. Hazard Mater.* **152**, 942–948.
- KHATIBI, A.D., MAHVI, A.H., MENGELIZADEH, N., & BALARAK, D. (2021). Adsorption–desorption of tetracycline onto molecularly imprinted polymer: isotherm, kinetics, & thermodynamics studies.
- LAGERGREN, S. (1898). About the theory of so-called adsorption of soluble substances, *Kungliga Svenska Vetenskapsakademiens H&lingar B&* **124**, 1–39.
- LANGMUIR, I. (1918). The adsorption of gases on plane surfaces of glass mica & platinum. *J. Am. Chem. Soc.* **40**, 1361–1402. <https://doi.org/10.1021/ja02242a004>
- LI, T., FAN, Y., CUN, D., DAI, Y., LIANG, W. (2020). Dibutyl phthalate adsorption characteristics using three common substrates in aqueous solutions. *Front. Environ. Sci. Eng.* 2020, **14**, 26 <https://doi.org/10.1007/s11783-019-1205-5>.
- MOUSAVI, S. A., ZANGENEH, H., ALMASI, A., NAYERI, D., MONKARESI, M., MAHMOUDI, A., & DARVISHI, P. (2020). Decolourization of aqueous methylene blue solutions by corn stalk: modeling & optimization. *Desalin. Water Treat.* **197**.
- MUNAGAPATI, V.S., YARRAMUTHI, V., KIM, Y., LEE, K.M., & KIM, D.S. (2018). Removal of anionic dyes (Reactive Black 5 & Congo Red) from aqueous solutions using Banana Peel Powder as an adsorbent. *Ecotoxicol. Environ. Saf.* **148**, 601–607.
- NIELSON, E., & LARSEN, P.B. (1996). Toxicological evaluation & limit values for DEHP & phthalates other than DEHP. *Danish Environ. Protect. Agency* **87**, 98.
- QI, J., LI, X., ZHENG, H., LI, P., & WANG, H. (2015). Simultaneous removal of methylene blue & copper (II) ions by photoelectron catalytic oxidation using stannic oxide modified iron (III) oxide composite electrodes. *J. Hazard. Mater.* **293**, 105–111.

- SADAF, S., & BHATTI, H.N. (2014). Batch & fixed bed column studies for the removal of Indosol Yellow BG dye by peanut husk. *J. Taiwan Inst. Chem. Eng.* **45**, 541–553.
- SAEED, A., SHARIF, M., & IQBAL, M. (2010). Application potential of grapefruit peel as dye sorbent: kinetics, equilibrium & mechanism of crystal violet adsorption. *J. Hazard. Mater.* **179**, 564–572.
- SCHOONENBERG KEGEL, F., RIETMAN, B.M., & VERLIEFDE, A.R.D. (2010). Reverse osmosis followed by activated carbon filtration for efficient removal of organic micropollutants from river bank filtrate. *Water Sci. Technol.* **61**, 2603–2610.
- SHEN, S., REN, J., CHEN, J., LU, X., DENG, C., & JIANG, X. (2011). Development of magnetic multiwalled carbon nanotubes combined with near-infrared radiation-assisted desorption for the determination of tissue distribution of doxorubicin liposome injects in rats. *J. Chromatogr. A* **1218**, 4619–4626.
- SINGH, D.K., & MISHRA, S. (2010). Synthesis & characterization of Hg (II)-ion-imprinted polymer: Kinetic & isotherm studies. *Desalination* **257**, 177–183. <https://doi.org/10.1016/j.desal.2010.02.026>
- TANG, X., HUANG, Y., HE, Q., WANG, Y., ZHENG, H., & HU, Y. (2021). Adsorption of tetracycline antibiotics by nitrilotriacetic acid modified magnetic chitosan-based microspheres from aqueous solutions. *Environ. Technol. Innov.* **24**, 101895.
- TEMKIN, M. I., & PYZHEV, V. (1940). Kinetics of ammonia synthesis on promoted iron catalysts. *Acta Physiochim.* **12**, 217–222.
- VASAPOLLO, G., DEL SOLE, R., MERGOLA, L., LAZZOLI, M.R., SCARDINO, A., SCORRANO, S., & MELE, G. (2011). Molecularly imprinted polymers: present & future prospective. *Int. J. Mol. Sci.* **12**, 5908–5945.
- WEBER, W.J., & MORRIS, J.S. (1963). Kinetics of adsorption on carbon from solutions. *J. Sanit. Eng. Div. Am. Soc. Civ. Eng.* **89**, 31–59.
- YAKUN, H., ET AL., (2011). Fluoride removal by lanthanum alginate bead: adsorbent characterization & adsorption mechanism. *Chin. J. Chem. Eng.* **19**, 365–370
- YONGFENG, K., WUPING, D., YAN, L., JUNXIA, K., & JING, X. (2012). Molecularly imprinted polymers of allyl- β -cyclodextrin & methacrylic acid for the solid-phase extraction of phthalate. *Carbohydrate Polymers* **88**, 459–464.
- ZHAO, C., DENG, H., LI, Y., & LIU, Z. (2010). Photodegradation of oxytetracycline in aqueous by 5A & 13X loaded with TiO₂ under UV irradiation. *J. Hazard. Mater.* **176**, 884–892.

Received 01 Sept 23; revised 07 March 24.